NIH Public Access
Author Manuscript
Biomaterials. Author manuscript; available in PMC 2015 March 01.

Published in final edited form as:
Biomaterials. 2014 March ; 35(9): 2868–2877. doi:10.1016/j.biomaterials.2013.12.030.

The role of mechanical tension on lipid raft dependent PDGF-induced TRPC6 activation

Lei Lei[a,b], **Shaoying Lu**[a,b], **Yi Wang**[a], **Taejin Kim**[a], **Dolly Mehta**[c], and **Yingxiao Wang**[a,b,*]

[a]Department of Bioengineering & Beckman Institute for Advanced Science and Technology, University of Illinois, Urbana-Champaign, Urbana, IL, 61801

[b]Department of Bioengineering & Institute of Engineering in Medicine, University of California, San Diego, La Jolla, CA, 92093

[c]Department of Pharmacology, College of Medicine, University of Illinois, Chicago, IL 60612

Abstract

Canonical transient receptor potential channel 6 (TRPC6) can play an important role in governing how cells perceive the surrounding material environment and regulate Ca^{2+} signaling. We have designed a TRPC6 reporter based on fluorescence resonance energy transfer (FRET) to visualize the TRPC6-mediated calcium entry and hence TRPC6 activity in live cells with high spatiotemporal resolutions. In mouse embryonic fibroblasts (MEFs), platelet-derived growth factor BB (PDGF) can activate the TRPC6 reporter, mediated by phospholipase C (PLC). This TRPC6 activation occurred mainly at lipid rafts regions of the plasma membrane because disruption of lipid raft/caveolae by methyl-β-cyclodextrin (MβCD) or the expression of dominant-negative caveolin-1 inhibited the TRPC6 activity. Culturing cells on soft materials or releasing the intracellular tension by ML-7 reduced this PDGF-induced activation of TRPC6 without affecting the PDGF-regulated Src or inositol 1,4,5-trisphosphate (IP_3) receptor function, suggesting a specific role of mechanical tension in regulating TRPC6. We further showed that the release of intracellular tension had similar effect on the diffusion coefficients of TRPC6 and a raft marker, confirming a strong coupling between TRPC6 and lipid rafts. Therefore, our results suggest that the TRPC6 activation mainly occurs at lipid rafts, which is regulated by the mechanical cues of surrounding materials.

Keywords

Fluorescence resonance energy transfer (FRET); Canonical transient receptor potential 6 (TRPC6); lipid rafts; intracellular tension; mechanical microenvironment

© 2013 Elsevier Ltd. All rights reserved

*To whom correspondence should be addressed. Yingxiao Wang, Ph. D. Department of Bioengineering & Institute of Engineering in Medicine, University of California, San Diego, La Jolla, CA, 92093 Tel: (858) 822-4502 Fax: (858) 822-1160 yiw015@eng.ucsd.edu.

Publisher's Disclaimer: This is a PDF file of an unedited manuscript that has been accepted for publication. As a service to our customers we are providing this early version of the manuscript. The manuscript will undergo copyediting, typesetting, and review of the resulting proof before it is published in its final citable form. Please note that during the production process errors may be discovered which could affect the content, and all legal disclaimers that apply to the journal pertain.

Author contributions L.L. and Yx.W. designed research; L.L., Y.W., and T.K. performed research; L.L. and S.L. analyzed data; and L.L., S.L., D.M. and Yx.W. wrote the paper.
The authors declare no conflict of interest.

NIH-PA Author Manuscript
NIH-PA Author Manuscript
NIH-PA Author Manuscript

NIH-PA Author Manuscript

NIH-PA Author Manuscript

NIH-PA Author Manuscript

1. Introduction

Intracellular calcium $(Ca^{2+})_i$ is a ubiquitous and crucial intracellular signal responsible for controlling numerous cellular processes including cell proliferation, differentiation, transcription factor activation and apoptosis [1]. Two sources are available for elevating $(Ca^{2+})_i$. The endoplasmic reticulum (ER) or the sarcoplasmic reticulum (SR) in muscle cells can serve as the intracellular source of $(Ca^{2+})_i$. Ca^{2+} can be released from ER or SR into the cytoplasm through the activation of IP_3 receptor on the ER membrane to increase $(Ca^{2+})_i$. The influx of Ca^{2+} from extracellular space through calcium channels on the plasma membrane is another source for $(Ca^{2+})_i$ elevation [1].

A novel superfamily of non-selective cation channels ion channels, transient receptor potential (TRP) channels, have been discovered to regulate $(Ca^{2+})_i$ by controlling Ca^{2+} entry from extracellular space [2]. Among this TRP superfamily, seven members of the mammalian TRPC subfamily have been characterized in human cells. Each TRPC member consists of six transmembrane spanning helices (TM1-6), connecting to cytoplasmic N and C termini, and forming a pore region between TM5 and TM6. Specially, TRPC3, TRPC6, and TRPC7 can assemble into homo- or hetero-tetramers that are crucial for various physiological consequences and activatible by a receptor-dependent activation process [2]. TRPC6 was further shown to play an important role in many pathological processes, such as lung injury, cardiovascular diseases, neuronal diseases and kidney disorder [3–7]. Particularly, high TRPC6 activity is related to cancer metastasis. Expression of TRPC6 was highly up-regulated in live cancer, breast cancer and glioma cells [8–10]; overexpression of TRPC6 can increase the proliferation of human hepatoma cells [8]. In contrast, inhibition of TRPC6 results in a significant reduction in cancer cells amplification and tumor growth [9, 10].

TRPC6 has also been shown to be involved in mechanotransduction. In fact, TRPC6 was found to contribute to pressure induced vasoconstriction and mediate mechanical hyperalgesia, synergistically with TRPV4 [11, 12]. TRPC6 can also mediate the synergistic effect of receptor and mechanical activations [13]. While direct activations of TRPC6 by membrane stretch was reported [14], it remains controversial whether TRPC6 is a direct mechanosensor or it cooperates with other sensing elements for the mechanotransduction [15].

Living cells are continuously exposed to environmental cues of surrounding materials. It becomes clear that mechanical microenvironment plays crucial roles in regulating cellular functions [16]. In fact, mechanical properties of a tissue can affect cancer progression [17]. Matrix rigidity also regulates cellular metabolisms for cell proliferation and stem cell differentiation [18, 19]. Furthermore, increasing substrate stiffness can enhance the sensitivity of fibroblasts to transforming growth factor β stimulation and facilitate their differentiation to myofibroblasts [20]. However it remains unclear how cells perceive the environmental cues of surrounding biomaterials and mediate the transmission of mechanical forces.

To monitor the function of TRPC6 in space and time, we will develop a FRET reporter specific to TRPC6 activation. We will then apply this reporter to investigate the TRPC6 activation at different submembrane microdomains. The effect of mechanical environment on the TRPC6 function will also be studied to understand how cells perceive the environmental cues and regulate intracellular molecular functions.

NIH-PA Author Manuscript

NIH-PA Author Manuscript

NIH-PA Author Manuscript

2. Materials and Methods

2.1. Reagents

Fetal bovine serum was obtained from Atlanta Biologicals (Lawrenceville, USA). 1-Oleoyl-2-acetyl-sn-glycerol (OAG), BAPTA, FITC conjugate cholera toxin B subunit (FITC-CTxB), methyl-beta-cyclodextrin (MβCD), ML-7, rat recombinant platelet-derived growth factor BB (PDGF), Thapsigargin (TG), and U-73122 were from Sigma Aldrich (Milwaukee, USA). The constructs pEYFP-TRPC6 and pEGFP-Caveolin-1 were shown in previous publications [21]. The plasmid cameleon Ca^{2+} reporter D3cpv was a generous gift from Dr. Amy E. Palmer (Department of Chemistry and Biochemistry, University of Colorado).

2.2. Cell culture and transfection

Mouse embryonic fibroblasts (MEFs) and HEK293T cells were from American Type Culture Collection (ATCC). Bovine aortic endothelial cells (BAECs) were isolated from bovine aorta from a local slaughterhouse as described [22]. Approval for handling BAECs was granted by the Institutional Review Board of University of Illinois, Urbana-Champaign. The cells were cultured in high glucose of Dulbecco's Modified Eagle Medium (DMEM, GIBCO, Invitrogen, USA) containing 10% fetal bovine serum, 2 mM L-glutamine, 100 unit/ml penicillin and 100 μg/ml sodium pyruvate in a humidified incubator of 95% O_2 and 5% CO_2 at 37°C. The DNA plasmids were transfected into the cells by using Lipofectamine 2000 (Invitrogen).

2.3. Construction of plasmids

The TRPC6 reporter was constructed by fusing human TRPC6 coding sequence with cameleon Ca^{2+} reporter D3cpv coding sequence. The human TRPC6 coding sequence was amplified by PCR with a sense primer containing a BamH I site and a reverse primer containing the coding sequence of a 17mer linker GSTSGSGKPGSGEGSTK and an EcoR I site. The PCR product was cloned into pcDNA3.1 (Invitrogen) using BamH I/EcoR I sites. Because of the similar DNA sequence of enhanced cyan fluorescent protein (ECFP) and circularly permutated Venus (cpVenus), the coding sequence of cameleon Ca^{2+} biosensor D3cpv was separated into 2 pieces by Bgl II digestion. These 2 pieces were amplified separately by PCR with a sense primer containing an EcoR I site and a reverse primer containing a Bgl II site for the first piece, and a sense primer containing a Bgl II site and a reverse primer containing a Not I site for the second piece. The PCR products were fused together and cloned into pcDNA3.1, fused at the C-terminal of TRPC6 after the 17mer linker. The human Caveolin-1 coding sequence was amplified by PCR with a sense primer containing a BamH I site and a reverse primer containing an EcoR I site, and cloned into pcDNA3.1 using BamH I/EcoR I sites. To generate a membrane-targeted cameleon Ca^{2+} reporter, the acylation substrate sequences derived from lyn kinase (MGCIKSKRKDNLNDDGVDMKT) was added to the N terminus [23], and a prenylation substrate sequence (KKKKKKSKTKCVIM) from KRas was added to the C terminus of the cytosolic reporter [24, 25].

FRET-ER calcium biosensor was constructed by fusion of calreticulin signal sequence (MLLPVLLLGLLGAAAD) and ER retension sequence (KDEL) to the N-terminus and the C-terminus of the cytosolic calcium reporter D3cpv, respectively.

The mutated TRPC6 reporter and the dominant-negative Caveolin-1 mutant were generated by using QuikChange® Site-Directed Mutagenesis Kit (Stratagene). Restriction enzyme digestion and DNA sequencing were applied to confirm all the constructed plasmids.

NIH-PA Author Manuscript

NIH-PA Author Manuscript

NIH-PA Author Manuscript

2.4 Flow system

To impose a laminar flow on HEK293T or BAECs, a parallel-plate flow chamber was applied as previously described [26–28]. In brief, a glass slide seeded with cells forms the floor of a flow channel, created by sandwiching a silicone gasket between the cover glass slide and an acrylic plate. Cells are exposed to a high shear stress (HSS) created by flows originated from a hydrostatic pressure difference between two reservoirs positioned with different heights. The channel width is 10 mm, channel height 0.5 mm, the total and entrance lengths are 45 and 15 mm, respectively. This flow chamber system has been well established to apply precisely controlled wall shear stress, which can be calculated as: $\tau_w = \frac{6\mu Q}{h^2 w}$, where μ = fluid viscosity of solution, Q = flow rate, h = channel height, w = channel width. This flow system was perfused with medium containing polystyrene particles to confirm the laminar flow patterns. HSS was set to be 65 dyn/cm^2 as previously described [28]. The flow experiments were conducted at 37 °C with 5% CO_2 to maintain the pH at 7.4.

Polyacrylamide gel preparation—The polyacrylamide gel dishes were prepared according to a well-established protocol [29], with the following component: 3% acrylamide (40% solution stock, Bio-Rad), 0.06% bis-acrylamide (2% solution stock, Bio-Rad), 1:200 10% w/v Amonium Persulfate (Bio-Rad) and 1:2000 N,N,N9,N9-Tetramethylethylenediamine (TEMED; Bio-Rad) in 10 mM HEPES buffer (Sigma). The stiffness of the gels was 0.6 kPa approximately. N-Sulfosuccinimidyl-6-(4'-azido-2'-nitrophenylamino) hexanoate (Sulfo-SANPAH) (Thermo Scientific) was used to crosslink extracellular matrix proteins onto the gel surface as previously described [30].

2.5. Image acquisition and analysis

Cells were plated on glass bottom dishes (Cell E&G Inc.) or gel dishes coated with 20 μg/ml fibronectin and cultured for 36–48 h in medium with 0.5% FBS before growth factor stimulation, or in medium with 10% FBS before OAG stimulation. During imaging process, the cells were maintained in CO_2-independent medium (Gibco BRL) with 0.5% FBS for growth factor stimulation, or with 10% FBS for OAG stimulation at 37°C. Images were collected by a Zeiss axiovert inverted microscope equipped with a cooled charge-coupled device camera (Cascade 512B; Photometrics) using MetaFluor 6.2 software (Universal Imaging) with a 420DF20 excitation filter, a 450DRLP dichroic mirror, and two emission filters controlled by a filter changer (475DF40 for ECFP channel and 535DF25 for FRET (YFP) channel of cpVenus and YPet). The proper regions were selected as the regions of interests to collect signals and conduct quantification. The fluorescence intensity of non-transfected cells were quantified as the background signal and subtracted from the ECFP and FRET (YFP) signals on transfected cells. Hence, the pixel-by-pixel ratio images of ECFP and FRET (YFP) were calculated based on the background-subtracted fluorescence intensity images of ECFP and FRET (YFP) by the MetaFluor software to represent the activation level of reporters.

Statistical analysis was performed by using a Student's t test function of the Excel software (Microsoft) to evaluate the statistical difference between groups. A significant difference was determined by P value (<0.05).

For confocal imaging, MEFs were transfected with TRPC6-mcherry. After culturing for 36 to 48 h, MEFs were washed with PBS and incubated with 1 μg/ml FITC-CTxB for 30 min, and washed with cold PBS twice before being fixed with 4% paraformaldehyde for 20 min. The images were recorded under confocal microscope.

NIH-PA Author Manuscript

NIH-PA Author Manuscript

NIH-PA Author Manuscript

2.6. Photobleaching assay and diffusion Analysis

MEFs were transfected with TRPC6-YFP or empty vector. Transfected cells were then plated on glass bottom dishes and cultured for 36–48 h in medium with 0.5% FBS before imaging experiments. MEFs transfected with empty vectors were stained with 1 μg/ml FITC-CTxB for 30 min at 37°C in culture medium containing 0.5% FBS. Cells were pretreated with or without 5 μM ML-7 for 1 hr before imaging. Images were collected by a Zeiss axiovert inverted microscope with a 495DF20 excitation filter, a 510 DCLP dichroic mirror, and a 535DF25 emission filters for YFP emission. During imaging, the cells were kept in CO_2-independent medium with 0.5% FBS at 37°C and monitored at 10-second intervals before and after photobleaching. Photobleaching was conducted by exciting YFP at 495DF20 in a region of interest with full power of the light source for 10 seconds.

The diffusion analysis procedure was described in our previous publication [31]. Specifically, the intensity images were normalized by dividing the median of five images before photobleaching to calculate the ratio images which represent the relative concentration maps of the fluorescent proteins. The concentration maps were then filtered by a 100×100 (15 μm × 15μm) local adaptive filter restricted within a cell body detected by the segmentation method [31]. As a result, the concentration maps before photobleaching had values close to 1 at all pixels within the cell, while those after photobleaching had values <1 near the photobleached region. Seven filtered concentration maps right after photobleaching were used to estimate 6 values of diffusion coefficients. Since the fluorescent proteins are expected to diffuse during photobleaching as well as recovery phases, a mobile subcellular region can be determined by selecting the subcellular region where the concentration decreases right after photobleaching. Thus, within the selected mobile subcellular region, the movement of the fluorescent proteins can be modeled by Fick's Law of diffusion [31]. The concentration maps within the shape of the cells were discretized using the finite element method with a triangular mesh to obtain a linear model of “the weighted discrete Laplacian of concentration” and “the weighted change of concentration in time” as described previously [31]. By linear regression, a diffusion coefficient *D* can be estimated with a residual r and the correlation coefficient R which measures the quality of regression. A value of R no less than 0.5 is considered as a good fit [31]. The corresponding diffusion coefficients, *D*, were then entered in the statistical comparison. The mean values of diffusion coefficients from different groups were compared with one-tailed t-test of unequal variance. P-value<=0.05 was considered significant difference. The fluorescence intensity images were all background subtracted, filtered by a 3×3 median filter and cropped before processing. It was also confirmed that the cell shape did not change significantly within the 110 sec when the images before or after photobleaching were collected.

3. Results

3.1. The Development and Characterization of TRPC6 reporter

To monitor the activity of TRPC6, the cameleon calcium reporter D3cpv [32] was fused at the C terminal of TRPC6 to monitor the local calcium influx mediated by TRPC6. When TRPC6 is activated, Ca^{2+} influx can elevate the local intracellular Ca^{2+} proximal to TRPC6 at the plasma membrane. This local Ca^{2+} can bind to calmodulin domain (CaM) of the D3cpv reporter which then binds to the intramolecular M13 domain with a high affinity. These events can lead to the conformational change of D3cpv reporter and enhance the FRET efficiency to result in the increase of FRET/cyan fluorescent protein (CFP) ratio (Fig. 1A). To characterize this engineered TRPC6 reporter, Human embryonic kidney 293T (HEK293T) cells which had minimal TRPC activity were transfected with wild type or mutated TRPC6 reporter. As shown in Fig. 1B–C and supplementary movie 1, a significant FRET change can be observed with the TRPC6 reporter within 10 min when cells are

NIH-PA Author Manuscript

NIH-PA Author Manuscript

NIH-PA Author Manuscript

exposed to an exogenous TRPC6 activator 1-Oleoyl-2-acetyl-sn-glycerol (OAG). In contrast, no FRET change can be observed (Fig. 1B–C and supplementary movie 1) with a mutated TRPC6 reporter in which the L678, F679, and W680 in the putative pore region of TRPC6 were replaced with alanine residues to eliminate the channel function [33]. We also incubated cells in a Ca^{2+} free extracellular solution and the FRET change of the wild-type TRPC6 reporter could not be detected (Fig. S1). Elimination of intracellular Ca^{2+} source by endoplasmic reticulum (ER) Ca^{2+} pump inhibitor thapsigargin (TG), on the other hand, did not block the activation of TRPC6 reporter (Fig. S2). These results suggest that the FRET signals are specifically dependent on the TRPC6 channel activity and extracellular Ca^{2+} influx. Similar results were observed in HEK293T cells co-expressing TRPC6 and a separate cytosolic D3cpv calcium reporter (Fig. 1D–E). Again, mutated TRPC6 did not cause the D3cpv response to OAG. HEK293T cells expressing D3cpv reporter alone failed to respond to OAG stimulation (Fig. 1D–E). These results confirmed that the exogenously expressed TRPC6 is the main source for the OAG-induced Ca^{2+} signaling and the FRET response of the reporter can monitor the TRPC6-controlled Ca^{2+} influx and hence TRPC6 functions in HEK293T cells.

3.2. TRPC6 can be activated by PDGF via PLC pathway in MEFs

Platelet-derived growth factor (PDGF) is well known to be involved in multiple cellular and developmental responses [34], by stimulating the increase of intracellular Ca^{2+} level [35]. Hence, we examined whether PDGF can induce the activation of TRPC6 in regulating signaling transduction in fibroblasts. We first confirmed that the wild type TRPC6 reporter but not mutated TRPC6 reporter responded to OAG stimulation in mouse embryonic fibroblasts (MEFs) (Fig. 2A). PDGF obviously caused the activation of TRPC6 (Fig. 2B and supplementary movie 2), independent of IP_3-mediated release of ER Ca^{2+} which was depleted by TG pretreatment (Fig. S3A). The effect of TG treatment was verified by blocking the ATP-induced calcium signaling in cells, which relied on the ER Ca^{2+} release (Fig. S3B). As expected, there was no response of TRPC6 reporter when MEFs were incubated in a Ca^{2+} free extracellular solution (Fig. S4).

It is well known that both PDGF receptors (PDGFR) engage several well-characterized signaling pathways, e.g. mitogen-activated protein kinases, phosphatidylinositide 3-kinases, and PLC [34]. As a downstream target, PLC binds to the phosphorylated PDGFRs to become activated [36]. The activation of PLC leads to the generation of diacylglycerol (DAG) which is an endogenous TRPC6 activator and of IP_3 which causes Ca^{2+} release from ER [1, 37]. To confirm whether the activation of TRPC6 induced by PDGF was through PLC pathway, MEFs were pretreated with PLC inhibitor U73122. The imaging results showed that U73122 almost completely blocked the activation of TRPC6 induced by PDGF (Fig. 2C), but not the OAG induced TRPC6 activation (Fig. 2D). Since IP_3 as another product of activated PLC can induce the ER Ca^{2+} release though IP_3 receptor [1], the cytoplasmic Ca^{2+} reporter D3cpv was applied to monitor the ER Ca^{2+} release and hence the production of IP_3 and the activation of PLC. Consistently, the increase of D3cpv activity induced by PDGF was also inhibited by U73122 (Fig. 2C); However, the activation of a direct effector of PDGFR, Src, which was detected by a KRas-Src reporter [25], was not affected by U73122 (Fig. 2C), confirming that U73122 specifically blocked PLC signaling without affecting the upstream Src activation upon PDGF stimulation. All these results indicate that PDGF specifically activated TRPC6 through PLC pathway.

3.3. Activation of TRPC6 depends on lipid rafts and caveolae

Lipid rafts are plasma membrane microdomains enriched in cholesterol and sphingolipids. Within lipid rafts, a specialized submembrane microdomain, caveolae are defined as caveolin-1-enriched smooth invaginations of the plasma membrane. Those microdomains

NIH-PA Author Manuscript

NIH-PA Author Manuscript

NIH-PA Author Manuscript

play crucial roles in compartmentalization of molecules and signal transduction [38]. TRPC proteins have been reported to be integral components of lipid rafts [39, 40]. However, it remains controversial since TRPC6 has been reported to be associated with caveolin 1/2 rich membrane fraction in HEK293T cells [41] but not in human platelets [42]. Here, we first monitored the Ca^{2+} influx across TRPC6 using two Ca^{2+} reporters with different sub-membrane localization. As shown in Fig. 3A, the Lyn-D3cpv reporter in lipid rafts region had obviously stronger response to the TRPC6-mediated Ca^{2+} influx than the KRas-D3cpv reporter in non-raft region upon OAG stimulation. In contrast, both the Lyn-D3cpv and KRas-D3cpv reporters had similar responses to the ER Ca^{2+} release induced by ATP (Fig. 3A). These results suggest that TRPC6 may be localized at lipid rafts to cause more significant Ca^{2+} alteration at these local sites. Consistently, the treatment of MβCD to extract the cholesterol from the plasma membrane and disrupt the lipid rafts blocked the activation of TRPC6 induced by OAG (Fig. 3B). This treatment also blocked the TRPC6 activation induced by PDGF (Fig. 3C). However, the activation of Src (detected by the KRas-Src reporter) and the production of IP_3 (detected by the D3cpv reporter) were not affected by the treatment of MβCD (Fig. 3C). Those results suggest that the disruption of lipid rafts only affects the activity of TRPC6 but not the upstream signaling pathway. We further studied the role of caveolae in the TRPC6 activation. A caveolin-1 dominant-negative mutant (Cav 1 S80E) was generated with S80E mutation which trapped the caveolin-1 in the ER to disrupt the caveolae structure [43]. The results showed that the co-expression of this dominate negative caveolin-1 inhibited the activation of TRPC6 induced by OAG (Fig. 3D) or PDGF (Fig. 3E). Again, the PDGF-induced upstream signals monitored by the KRas-Src reporter and the D3cpv reporter were not affected (Fig. 3E). The confocal images further showed that mcherry tagged-TRPC6 and rafts marker ganglioside GM1 stained with FITC conjugate cholera toxin B subunit (FITC-CTxB) had the similar location on the cell membrane (Fig. 3F). It is of note that a large number of TRPC6-mCherry is localized at peri-nuclear regions, possibly reflecting TRPC6-mCherry trapped in endo/exocytosis recycling routes before being correctly transported to the plasma membrane [44]. These results suggest that the functional TRPC6 channel can localize and function at the lipid raft/caveolae microdomains of the plasma membrane.

3.4. Substrate rigidity and intracellular tension affect TRPC6 activity

TRPC6 was reported to be activatable by mechanical force such as membrane stretch induced by hypotonicity [13, 14]. Thus we tested whether shear stress induced by laminar flow could activate TRPC6. However, in tested HEK293T cells and bovine aortic endothelial cells (BAECs), high shear stress (65 dyn/cm^2) failed to activate TRPC6 (Fig. 4A–B). We further examined the effect of mechanical microenvironment on TRPC6 activity by altering the stiffness of substrate materials. As shown in Fig. 4C, OAG induced markedly less TRPC6 reporter activity in MEFs cultured on the soft substrate (polyacrylamide gel with 600 pa stiffness) than MEFs cultured on hard glass surface. Similar results were observed when MEFs were stimulated with PDGF (Fig. 4D). In contrast, the upstream signals monitored by the KRas-Src and D3cpv reporter did not show any different response under different substrate rigidity (Fig. 4D). These results indicate that the substrate rigidity, which is known to modulate the intracellular tension [45, 46], affects TRPC6 function but not the upstream PDGF signaling molecules. A myosin light chain kinase inhibitor, ML-7 which can release the actomyosin contractility and intracellular tension also consistently inhibited the response of TRPC6 to the OAG and PDGF stimulation (Fig. 4E–F) without affecting the PDGF-induced Src and IP3 signaling pathways (Fig. 4F).

3.5. Intracellular tension affects TRPC6 dynamics

It is clear that the TRPC6 activity is regulated by intracellular tension. We hence investigated how intracellular tension affected TRPC6 functions. Fluorescence recovery

NIH-PA Author Manuscript

NIH-PA Author Manuscript

NIH-PA Author Manuscript

after photobleaching (FRAP) was applied to characterize the motion of TRPC6. A previously developed diffusion analysis method based on finite element discretization was also used to estimate the apparent diffusion coefficients of yellow fluorescent protein (YFP) fused TRPC6 [31]. The TRPC6-YFP of a small region of MEFs was photobleached (Fig. 5A). The post-bleaching images were monitored and then normalized by the pre-bleaching images to obtain concentration maps. Subsequently, the finite element analysis and linear regression method were applied to estimate apparent diffusion coefficient (Fig. 5B). As shown in Fig. 5C, the fluorescence intensity of the TRPC6-YFP partially recovered in 5 min after photobleaching. The mean diffusion coefficient of TRPC6 was 1.03 μm^2/sec which was similar to the rafts marker ganglioside GM1 (1.05 μm^2/sec), which was obtained using the FITC-CTxB labeled ganglioside GM1. Release of intracellular tension by ML7 obviously decreased the TRPC6 diffusion coefficient to 0.585 μm^2/sec as well as GM1 (0.605 μm^2/sec) (Fig. 5D).These results suggest that the release of intracellular tension may affect lipid raft/caveolae microdomains and hence regulate the TRPC6 function.

4. Discussion

In the current work, we have developed a FRET based TRPC6 reporter to visualize TRPC6 activity in live cells. With this reporter, PDGF is found to induce TRPC6 activation in a PLC-dependent manner. This activation occurs mainly at the lipid raft/caveolae microdomains of the plasma membrane, which is regulated by the intercellular tension. Therefore, this reporter provides a powerful tool to study the underlying molecular mechanisms that regulate TRPC6.

PDGF plays an important role in regulating the cellular activity of fibroblasts. One of the early cellular events upon PDGF stimulation is a rapid, transient elevation in intracellular Ca^{2+} level [47]. Inhibition of PDGF-induced Ca^{2+} elevation results in the inhibition of the mitogenic response [35]. TRPC6 activity is involved in the intracellular Ca^{2+} regulation by PDGF in glioma cells [10]. Using the TRPC6 FRET reporter, we provide direct evidence that PDGF can activate TRPC6 to trigger Ca^{2+} influx across the plasma membrane via PLC pathway in MEFs (Fig. 2B–C). Various and sometimes controversial regulatory mechanisms of TRPC6 have also been reported in response to PDGF. For example, PDGF can up-regulate TRPC6 expression to result in the stimulation of cell proliferation in pulmonary vascular smooth muscle cell [48]. However, knocking down of TRPC6 expression has no effect on the PDGF induced Ca^{2+} influx in vascular smooth muscle cells [49].

Fyn, a member of the Src family kinase, can interact with N-terminal cytoplasmic region of TRPC6 and cause the tyrosine phosphorylation of TRPC6 to increase TRPC6 channel activity in short terms [50]. On the other hand, TRPC6 channel activity can be negatively regulated by the Thr69 phosphorylation of the N-terminal region [51]. The membrane location of TRPC6 can also be affected by Gq protein-coupled receptor to regulate TRPC6 functions [41]. Our results clearly indicate that the PDGF-induced TRPC6 occurs at the lipid rafts of the plasma membrane (Fig. 3), which is dependent on the PLC pathway (Fig. 2C). These results are consistent with previous reports that TRPC6 was located in caveolin 1/2 rich membrane fraction in HEK293T cells [41] and MβCD can completely abolish the TRPC6-mediated intracellular Ca^{2+} elevation induced by DAG-containing arachidonic acids in HEK293T cells [52], although in human platelets, TRPC6 appears independent of lipid rafts [42].

The effect and mechanism by which mechanical forces are involved in the regulation of TRPC6 activity remain unclear and controversial. Atheroprone shear stress increases TRPC6 expression in human umbilical vascular endothelial cells [53]. GsMTx-4, a specific peptide inhibitor of mechanosensitive channels, prevents a membrane stretch activated non-selective

NIH-PA Author Manuscript

NIH-PA Author Manuscript

NIH-PA Author Manuscript

cation conductance mediated by TRPC6. Stretch was further shown to directly activate TRPC6 independent of PLC [14]. However, the protein expression level of TRPC6 in African green monkey kidney (COS) or Chinese hamster ovary (CHO) cells did not affect the mechano-sensitive current [15]. These results suggest that TRPC6 may not directly sense and mediate the effect of mechanical tension, but may serve as a regulator to facilitate the mechanotransduction. Indeed, chemical and mechanical stimulations have been shown to synergistically activate TRPC6 via phospholipase C/diacylglycerol and phospholipase A2/omega-hydroxylase/20-HETE pathways [13]. In our work, external mechanical loading such as shear stress even with high magnitude (65 dyn/cm^2) did not cause the TRPC6 response (Fig. 4A–B). However, substrate rigidity is apparently involved in regulating the TRPC6 function in response to chemical stimuli. Culturing cells on a soft matrix surface with 600 Pa Young's elastic modulus obviously reduced the response of TRPC6 induced by OAG and PDGF (Fig. 4C–D). The application of ML7 to release intracellular tension further confirmed the significant role of mechanical force in affecting TRPC6 functions (Fig. 4E–F), possibly via the manipulation of lipid rafts structures. Indeed, ML7 had similar effect in reducing the diffusion coefficients of both TRPC6 and lipid rafts marker ganglioside GM1 (Fig. 5D). Our results also showed that the cholesterol depletion by MβCD can inhibit the PDGF-induced TRPC6 activation (Fig. 3B–C). The intracellular tension may hence act upstream to modulate lipid rafts in controlling TRPC6 functions, possibly mediated by the interaction between actin cytoskeleton and lipid rafts composition parts, e.g. phosphoinositide lipids, PtdIns(4,5)P_2, filamin A, and/or caveolin-1 [54, 55].

G protein coupled receptors (GPCRs) have been reported to be activatable by mechanical force [56, 57], which then triggers $G\alpha_q$-PLC pathway upstream to TRPC6 [58]. Our results of TRPC6 inhibition by releasing intracellular tension under OAG stimulation suggest that the effect of mechanical tension on TRPC6 can be independent of PLC pathway (Fig. 4C–E), since OAG induced TRPC6 activation is not affected by the PLC inhibitor (Fig. 2D). Therefore, intracellular tension may regulate TRPC6 activity mainly by affecting lipid rafts microdomains without the involvement of GPCRs (Fig. 6).

It is clear that the TRPC6 activity is affected by the mechanical cues of surrounding materials. In fact, mechanical microenvironment has been established to modulate the biological properties of tumor cells. For example, culturing cancer cells on soft materials reduce their growth rate, metabolism, and motility [59, 60]. Since high TRPC6 activity is related to cancer growth [8–10], our finding should shed new lights on how the mechanical cues of surrounding materials and tissue environment can modulate the sensing responsibility of cancer cells toward chemical and biochemical stimulations.

5. Conclusion

In this study, we have designed and characterized a specific TRPC6 FRET reporter to detect Ca^{2+} influx mediated by TRPC6. Using this reporter, we found that PDGF can activate TRPC6 via PLC pathway. This activation was dependent on lipid raft/caveolae microdomains. Mechanical microenvironment also played a role in regulating TRPC6 function: culturing cells on soft substrate attenuated the activation of TRPC6 by releasing the intracellular tension and altering lipid rafts properties. These findings suggest a new mechanism of how cells perceive the mechanical cues of the surrounding materials and transmit them into membrane molecular activities. The TRPC6 reporter can also provide a powerful tool to study TRPC6 functions in live cells with high spatiotemporal resolutions.

Supplementary Material

Refer to Web version on PubMed Central for supplementary material.

NIH-PA Author Manuscript

NIH-PA Author Manuscript

NIH-PA Author Manuscript

Acknowledgments

We thank Dr. Amy E. Palmer for cameleon Ca^{2+} reporter D3cpv plasmid. This work is supported by grants from NIH HL098472 and NSF CBET0846429.

References

[1]. Berridge MJ, Lipp P, Bootman MD. The versatility and universality of calcium signalling. Nat Rev Mol Cell Biol. 2000; 1(1):11–21. [PubMed: 11413485]

[2]. Clapham DE, Runnels LW, Strubing C. The TRP ion channel family. Nat Rev Neurosci. 2001; 2(6):387–96. [PubMed: 11389472]

[3]. Nishida M, Onohara N, Sato Y, Suda R, Ogushi M, Tanabe S, et al. Galpha12/13-mediated up-regulation of TRPC6 negatively regulates endothelin-1-induced cardiac myofibroblast formation and collagen synthesis through nuclear factor of activated T cells activation. J Biol Chem. 2007; 282(32):23117–28. [PubMed: 17533154]

[4]. Tai Y, Feng S, Ge R, Du W, Zhang X, He Z, et al. TRPC6 channels promote dendritic growth via the CaMKIV-CREB pathway. J Cell Sci. 2008; 121(Pt 14):2301–7. [PubMed: 18559891]

[5]. Inoue R, Jensen LJ, Shi J, Morita H, Nishida M, Honda A, et al. Transient receptor potential channels in cardiovascular function and disease. Circ Res. 2006; 99(2):119–31. [PubMed: 16857972]

[6]. Tauseef M, Knezevic N, Chava KR, Smith M, Sukriti S, Gianaris N, et al. TLR4 activation of TRPC6-dependent calcium signaling mediates endotoxin-induced lung vascular permeability and inflammation. J Exp Med. 2012; 209(11):1953–68. [PubMed: 23045603]

[7]. Winn MP, Conlon PJ, Lynn KL, Farrington MK, Creazzo T, Hawkins AF, et al. A mutation in the TRPC6 cation channel causes familial focal segmental glomerulosclerosis. Science. 2005; 308(5729):1801–4. [PubMed: 15879175]

[8]. El Boustany C, Bidaux G, Enfissi A, Delcourt P, Prevarskaya N, Capiod T. Capacitative calcium entry and transient receptor potential canonical 6 expression control human hepatoma cell proliferation. Hepatology. 2008; 47(6):2068–77. [PubMed: 18506892]

[9]. Aydar E, Yeo S, Djamgoz M, Palmer C. Abnormal expression, localization and interaction of canonical transient receptor potential ion channels in human breast cancer cell lines and tissues: a potential target for breast cancer diagnosis and therapy. Cancer Cell Int. 2009; 9:23. [PubMed: 19689790]

[10]. Ding X, He Z, Zhou K, Cheng J, Yao H, Lu D, et al. Essential role of TRPC6 channels in G2/M phase transition and development of human glioma. J Natl Cancer Inst. 2010; 102(14):1052–68. [PubMed: 20554944]

[11]. Welsh DG, Morielli AD, Nelson MT, Brayden JE. Transient receptor potential channels regulate myogenic tone of resistance arteries. Circ Res. 2002; 90(3):248–50. [PubMed: 11861411]

[12]. Alessandri-Haber N, Dina OA, Chen X, Levine JD. TRPC1 and TRPC6 channels cooperate with TRPV4 to mediate mechanical hyperalgesia and nociceptor sensitization. J Neurosci. 2009; 29(19):6217–28. [PubMed: 19439599]

[13]. Inoue R, Jensen LJ, Jian Z, Shi J, Hai L, Lurie AI, et al. Synergistic activation of vascular TRPC6 channel by receptor and mechanical stimulation via phospholipase C/diacylglycerol and phospholipase A2/omega-hydroxylase/20-HETE pathways. Circ Res. 2009; 104(12):1399–409. [PubMed: 19443836]

[14]. Spassova MA, Hewavitharana T, Xu W, Soboloff J, Gill DL. A common mechanism underlies stretch activation and receptor activation of TRPC6 channels. Proc Natl Acad Sci U S A. 2006; 103(44):16586–91. [PubMed: 17056714]

[15]. Gottlieb P, Folgering J, Maroto R, Raso A, Wood TG, Kurosky A, et al. Revisiting TRPC1 and TRPC6 mechanosensitivity. Pflugers Arch. 2008; 455(6):1097–103. [PubMed: 17957383]

[16]. Wells RG. The role of matrix stiffness in regulating cell behavior. Hepatology. 2008; 47(4): 1394–400. [PubMed: 18307210]

[17]. Butcher DT, Alliston T, Weaver VM. A tense situation: forcing tumour progression. Nat Rev Cancer. 2009; 9(2):108–22. [PubMed: 19165226]

NIH-PA Author Manuscript

NIH-PA Author Manuscript

NIH-PA Author Manuscript

[18]. Assoian RK, Klein EA. Growth control by intracellular tension and extracellular stiffness. Trends Cell Biol. 2008; 18(7):347–52. [PubMed: 18514521]

[19]. Engler AJ, Sen S, Sweeney HL, Discher DE. Matrix elasticity directs stem cell lineage specification. Cell. 2006; 126(4):677–89. [PubMed: 16923388]

[20]. Li Z, Dranoff JA, Chan EP, Uemura M, Sevigny J, Wells RG. Transforming growth factor-beta and substrate stiffness regulate portal fibroblast activation in culture. Hepatology. 2007; 46(4): 1246–56. [PubMed: 17625791]

[21]. Kini V, Chavez A, Mehta D. A new role for PTEN in regulating transient receptor potential canonical channel 6-mediated Ca2+ entry, endothelial permeability, and angiogenesis. J Biol Chem. 2010; 285(43):33082–91. [PubMed: 20705603]

[22]. Wang Y, Miao H, Li S, Chen KD, Li YS, Yuan S, et al. Interplay between integrins and FLK-1 in shear stress-induced signaling. Am J Physiol Cell Physiol. 2002; 283(5):C1540–7. [PubMed: 12372815]

[23]. Wang Y, Botvinick EL, Zhao Y, Berns MW, Usami S, Tsien RY, et al. Visualizing the mechanical activation of Src. Nature. 2005; 434(7036):1040–5. [PubMed: 15846350]

[24]. Zacharias DA, Violin JD, Newton AC, Tsien RY. Partitioning of lipid-modified monomeric GFPs into membrane microdomains of live cells. Science. 2002; 296(5569):913–6. [PubMed: 11988576]

[25]. Seong J, Lu S, Ouyang M, Huang H, Zhang J, Frame MC, et al. Visualization of Src activity at different compartments of the plasma membrane by FRET imaging. Chem Biol. 2009; 16(1):48–57. [PubMed: 19171305]

[26]. Fillinger MF, Sampson LN, Cronenwett JL, Powell RJ, Wagner RJ. Coculture of endothelial cells and smooth muscle cells in bilayer and conditioned media models. J Surg Res. 1997; 67(2):169–78. [PubMed: 9073564]

[27]. Nackman GB, Fillinger MF, Shafritz R, Wei T, Graham AM. Flow modulates endothelial regulation of smooth muscle cell proliferation: a new model. Surgery. 1998; 124(2):353–60. discussion 60–1. [PubMed: 9706159]

[28]. Liu B, Lu S, Zheng S, Jiang Z, Wang Y. Two distinct phases of calcium signalling under flow. Cardiovasc Res. 2011; 91(1):124–33. [PubMed: 21285296]

[29]. Pelham RJ Jr. Wang Y. Cell locomotion and focal adhesions are regulated by substrate flexibility. Proc Natl Acad Sci U S A. 1997; 94(25):13661–5. [PubMed: 9391082]

[30]. Kim TJ, Seong J, Ouyang M, Sun J, Lu S, Hong JP, et al. Substrate rigidity regulates Ca2+ oscillation via RhoA pathway in stem cells. J Cell Physiol. 2009; 218(2):285–93. [PubMed: 18844232]

[31]. Lu S, Ouyang M, Seong J, Zhang J, Chien S, Wang Y. The spatiotemporal pattern of Src activation at lipid rafts revealed by diffusion-corrected FRET imaging. PLoS Comput Biol. 2008; 4(7):e1000127. [PubMed: 18711637]

[32]. Palmer AE, Giacomello M, Kortemme T, Hires SA, Lev-Ram V, Baker D, et al. Ca2+ indicators based on computationally redesigned calmodulin-peptide pairs. Chem Biol. 2006; 13(5):521–30. [PubMed: 16720273]

[33]. Hofmann T, Schaefer M, Schultz G, Gudermann T. Subunit composition of mammalian transient receptor potential channels in living cells. Proc Natl Acad Sci U S A. 2002; 99(11):7461–6. [PubMed: 12032305]

[34]. Andrae J, Gallini R, Betsholtz C. Role of platelet-derived growth factors in physiology and medicine. Genes Dev. 2008; 22(10):1276–312. [PubMed: 18483217]

[35]. Wang Z, Estacion M, Mordan LJ. Ca2+ influx via T-type channels modulates PDGF-induced replication of mouse fibroblasts. Am J Physiol. 1993; 265(5 Pt 1):C1239–46. [PubMed: 8238477]

[36]. Tallquist M, Kazlauskas A. PDGF signaling in cells and mice. Cytokine Growth Factor Rev. 2004; 15(4):205–13. [PubMed: 15207812]

[37]. Hofmann T, Obukhov AG, Schaefer M, Harteneck C, Gudermann T, Schultz G. Direct activation of human TRPC6 and TRPC3 channels by diacylglycerol. Nature. 1999; 397(6716):259–63. [PubMed: 9930701]

NIH-PA Author Manuscript

NIH-PA Author Manuscript

NIH-PA Author Manuscript

[38]. Simons K, Toomre D. Lipid rafts and signal transduction. Nat Rev Mol Cell Biol. 2000; 1(1):31–9. [PubMed: 11413487]

[39]. Lockwich TP, Liu X, Singh BB, Jadlowiec J, Weiland S, Ambudkar IS. Assembly of Trp1 in a signaling complex associated with caveolin-scaffolding lipid raft domains. J Biol Chem. 2000; 275(16):11934–42. [PubMed: 10766822]

[40]. Lockwich T, Singh BB, Liu X, Ambudkar IS. Stabilization of cortical actin induces internalization of transient receptor potential 3 (Trp3)-associated caveolar Ca2+ signaling complex and loss of Ca2+ influx without disruption of Trp3-inositol trisphosphate receptor association. J Biol Chem. 2001; 276(45):42401–8. [PubMed: 11524429]

[41]. Cayouette S, Lussier MP, Mathieu EL, Bousquet SM, Boulay G. Exocytotic insertion of TRPC6 channel into the plasma membrane upon Gq protein-coupled receptor activation. J Biol Chem. 2004; 279(8):7241–6. [PubMed: 14662757]

[42]. Brownlow SL, Sage SO. Transient receptor potential protein subunit assembly and membrane distribution in human platelets. Thromb Haemost. 2005; 94(4):839–45. [PubMed: 16270640]

[43]. Schlegel A, Arvan P, Lisanti MP. Caveolin-1 binding to endoplasmic reticulum membranes and entry into the regulated secretory pathway are regulated by serine phosphorylation. Protein sorting at the level of the endoplasmic reticulum. J Biol Chem. 2001; 276(6):4398–408. [PubMed: 11078729]

[44]. Wiley HS, Burke PM. Regulation of receptor tyrosine kinase signaling by endocytic trafficking. Traffic. 2001; 2(1):12–8. [PubMed: 11208164]

[45]. Saez A, Buguin A, Silberzan P, Ladoux B. Is the mechanical activity of epithelial cells controlled by deformations or forces? Biophys J. 2005; 89(6):L52–4. [PubMed: 16214867]

[46]. Schwartz MA. Integrins and extracellular matrix in mechanotransduction. Cold Spring Harb Perspect Biol. 2010; 2(12):a005066. [PubMed: 21084386]

[47]. Moolenaar WH, Tertoolen LG, de Laat SW. Growth factors immediately raise cytoplasmic free Ca2+ in human fibroblasts. J Biol Chem. 1984; 259(13):8066–9. [PubMed: 6610677]

[48]. Yu Y, Sweeney M, Zhang S, Platoshyn O, Landsberg J, Rothman A, et al. PDGF stimulates pulmonary vascular smooth muscle cell proliferation by upregulating TRPC6 expression. Am J Physiol Cell Physiol. 2003; 284(2):C316–30. [PubMed: 12529250]

[49]. Bisaillon JM, Motiani RK, Gonzalez-Cobos JC, Potier M, Halligan KE, Alzawahra WF, et al. Essential role for STIM1/Orai1-mediated calcium influx in PDGF-induced smooth muscle migration. Am J Physiol Cell Physiol. 2010; 298(5):C993–1005. [PubMed: 20107038]

[50]. Hisatsune C, Kuroda Y, Nakamura K, Inoue T, Nakamura T, Michikawa T, et al. Regulation of TRPC6 channel activity by tyrosine phosphorylation. J Biol Chem. 2004; 279(18):18887–94. [PubMed: 14761972]

[51]. Nishida M, Watanabe K, Sato Y, Nakaya M, Kitajima N, Ide T, et al. Phosphorylation of TRPC6 channels at Thr69 is required for anti-hypertrophic effects of phosphodiesterase 5 inhibition. J Biol Chem. 2010; 285(17):13244–53. [PubMed: 20177073]

[52]. Aires V, Hichami A, Boulay G, Khan NA. Activation of TRPC6 calcium channels by diacylglycerol (DAG)-containing arachidonic acid: a comparative study with DAG-containing docosahexaenoic acid. Biochimie. 2007; 89(8):926–37. [PubMed: 17532549]

[53]. Thilo F, Vorderwulbecke BJ, Marki A, Krueger K, Liu Y, Baumunk D, et al. Pulsatile atheroprone shear stress affects the expression of transient receptor potential channels in human endothelial cells. Hypertension. 2012; 59(6):1232–40. [PubMed: 22566504]

[54]. Caroni P. New EMBO members' review: actin cytoskeleton regulation through modulation of PI(4,5)P(2) rafts. EMBO J. 2001; 20(16):4332–6. [PubMed: 11500359]

[55]. Stahlhut M, van Deurs B. Identification of filamin as a novel ligand for caveolin-1: evidence for the organization of caveolin-1-associated membrane domains by the actin cytoskeleton. Mol Biol Cell. 2000; 11(1):325–37. [PubMed: 10637311]

[56]. Yasuda N, Akazawa H, Qin Y, Zou Y, Komuro I. A novel mechanism of mechanical stress-induced angiotensin II type 1-receptor activation without the involvement of angiotensin II. Naunyn Schmiedebergs Arch Pharmacol. 2008; 377(4–6):393–9. [PubMed: 18046542]

NIH-PA Author Manuscript

NIH-PA Author Manuscript

NIH-PA Author Manuscript

[57]. Mederos y Schnitzler M, Storch U, Meibers S, Nurwakagari P, Breit A, Essin K, et al. Gq-coupled receptors as mechanosensors mediating myogenic vasoconstriction. EMBO J. 2008; 27(23):3092–103. [PubMed: 18987636]

[58]. Singh I, Knezevic N, Ahmmed GU, Kini V, Malik AB, Mehta D. Galphaq-TRPC6-mediated Ca2+ entry induces RhoA activation and resultant endothelial cell shape change in response to thrombin. J Biol Chem. 2007; 282(11):7833–43. [PubMed: 17197445]

[59]. Tilghman RW, Blais EM, Cowan CR, Sherman NE, Grigera PR, Jeffery ED, et al. Matrix rigidity regulates cancer cell growth by modulating cellular metabolism and protein synthesis. PLoS One. 2012; 7(5):e37231. [PubMed: 22623999]

[60]. Ananthanarayanan B, Kim Y, Kumar S. Elucidating the mechanobiology of malignant brain tumors using a brain matrix-mimetic hyaluronic acid hydrogel platform. Biomaterials. 2011; 32(31):7913–23. [PubMed: 21820737]

NIH-PA Author Manuscript

NIH-PA Author Manuscript

NIH-PA Author Manuscript

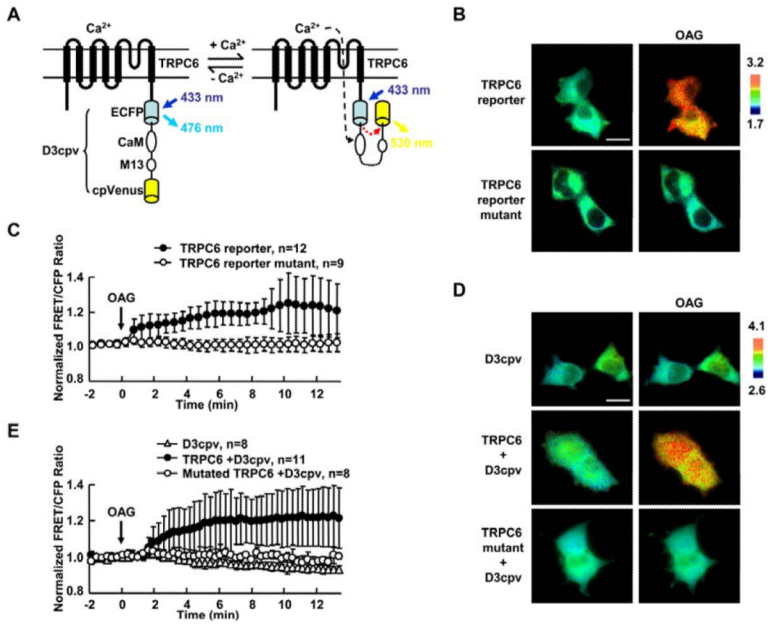

Fig. 1. The characterization of the TRPC6 FRET reporter

(**A**) The domain structure of the TRPC6 FRET reporter. This reporter includes a full length human TRPC6 with a cameleon Ca^{2+} reporter D3cpv at its C terminus. Cyan column and arrow presents ECFP and its emission; yellow column and arrow presents cpVenus and its emission, respectively. (**B**) and (**D**) FRET/CFP ratio images of HEK293T cells before (left) and after (right) 10 min stimulation by 100 μM OAG. HEK293T cells were transfected with (**B**) the wild type and mutant TRPC6 reporter or (**D**) the cameleon D3cpv reporter, wild type or mutant TRPC6 expression construct with D3cpv reporter as indicated. In all the panels, the color scale bars represent the FRET/CFP emission ratio, with cold and hot colors representing low and high activities of reporter, respectively. (**C**) and (**E**) Representative time courses of normalized FRET/CFP emission ratio of (**C**) TRPC6 reporter (black dots) and its mutant (white dots) or (**E**) D3cpv reporter (D3cpv plus empty vector, triangle; D3cpv plus wild type TRPC6, black dots; and D3cpv plus mutant TRPC6, white dots) before and after OAG stimulation, including cells from (**B**) or (**D**), respectively. 100 μM OAG was added at time 0 as indicated. The time courses represent the means±SD of each time point from multi-samples by setting the average FRET/CFP ratio of time points before stimulation to 1.0; “n” represents the cell number in each group. Size scale bar, 20 μm.

NIH-PA Author Manuscript

NIH-PA Author Manuscript

NIH-PA Author Manuscript

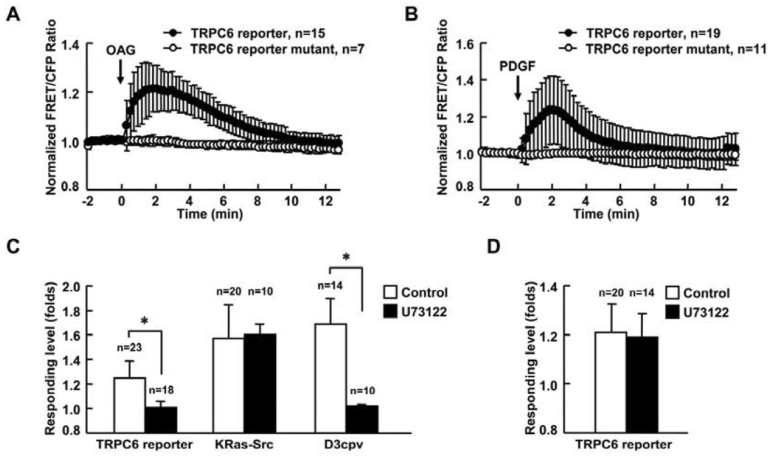

Fig. 2. PDGF activates TRPC6 via the PLC pathway in MEFs

(**A**) and (**B**) Representative time courses of normalized FRET/CFP emission ratio of TRPC6 reporter (black dots) and its mutant (white dots) upon (**A**) 300 μM OAG or (**B**) 10 ng/ml PDGF stimulation. (**C**) Responses of TRPC6, KRas-Src or D3cpv reporter to 10 ng/ml PDGF stimulation in MEFs with (solid bars) or without (open bars) 2 μM U73122 pretreatment for 5 min. MEFs transfected with the TRPC6 reporter were pretreated with 1 μM TG for 1 hr before imaging to deplete the calcium storage ofintracellular organelles. MEFs transfected with D3cpv were maintained in Ca^{2+} free HBSS buffer during imaging to eliminate the calcium influx across the plasma membrane. (**D**) Responses of TRPC6 reporter to 300 μM OAG stimulation in MEFs with or without 2μM U73122 pretreatment for 5 min. The data represents the means±SD from multi-samples. “n” represents the cell number in each group. * indicates the significant difference between indicated groups ($P < 0.01$).

NIH-PA Author Manuscript

NIH-PA Author Manuscript

NIH-PA Author Manuscript

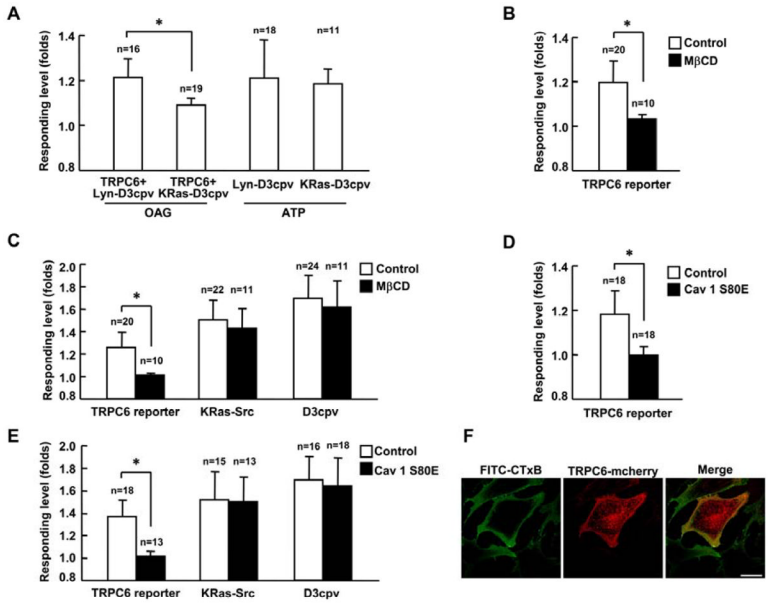

Fig. 3. The activation of TRPC6 depends on lipid rafts and caveolae

(**A**) Responses of Lyn-D3cpv and KRas-D3cpv reporters upon 100 μM OAG or 10 nM ATP stimulation as indicated. Lyn-D3cpv or KRas-D3cpv reporter was transfected into HEK293T cells with (OAG stimulation) or without the co-transfection of wild type TRPC6 (ATP stimulation) as indicated. (**B**) and (**D**) Response of TRPC6 reporter to 100 μM OAG stimulation in HEK239T cells (**B**) with 10 μM MβCD pretreatment or (**D**) with the expression of dominate negative Caveolin-1 (Cav 1 S80E). MbCD was added into medium 1 hr before stimulation with OAG. (**C**) and (**E**) Responses of TRPC6, KRas-Src or D3cpv reporter to 10 ng/ml PDGF stimulation in MEFs (**C**) with 10 μM MβCD pretreatment or (**E**) with the expression of Cav1 S80E. MEFs transfected with TRPC6 reporter were pretreated with 1 μM TG for 1 hr before imaging. MEFs transfected with the D3cpv reporter were maintained in Ca^{2+} free HBSS buffer during imaging. (**F**) Confocal images of FITC-CTxB labeled ganglioside GM1 and TRPC6-mCherry in MEFs. “n” represents the cell number in each group. * indicates the significant difference between indicated groups ($P < 0.01$). Scale bar, 25 μm.

NIH-PA Author Manuscript

NIH-PA Author Manuscript

NIH-PA Author Manuscript

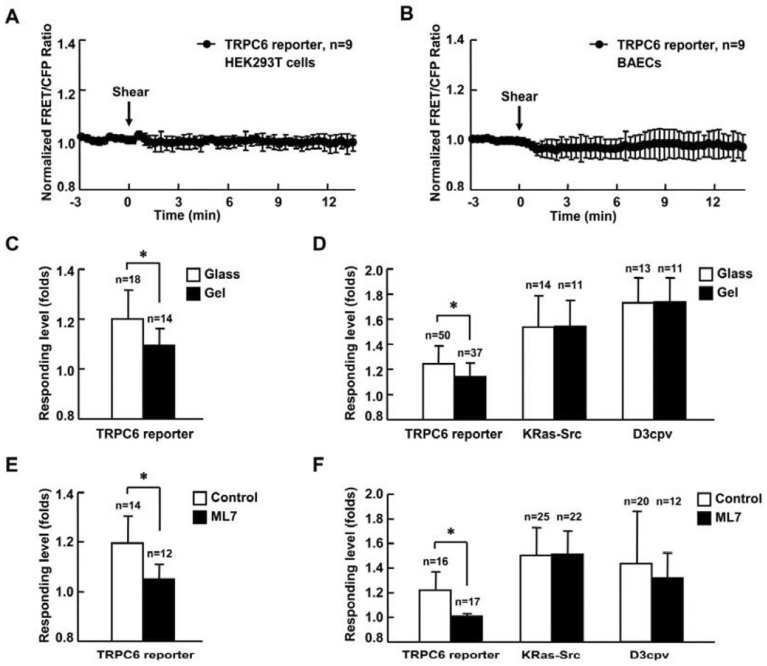

Fig. 4. Substrate rigidity and intercellular tension affect TRPC6 activity

(**A**) and (**B**) Representative time courses of normalized FRET/CFP emission ratio of TRPC6 reporter inresponse to 65 dyn/cm^2 shear stress stimulation (time 0) in HEK293T cells (**A**) or BAECs (**B**). (**C**) and (**E**) Response of TRPC6 reporter to 300 μM OAG stimulation in MEFs (**C**) cultured on rigid surface (glass) or soft substrate (gel with 600 pa stiffness) or (**E**) with 5 μM ML-7 pretreatment for 1hr. (**D**) and (**F**) Responses of TRPC6, KRas-Src, or D3cpv reporter to 10 ng/ml PDGF stimulation in MEFs (**D**) cultured on rigid surface (glass) or soft substrate (gel with 600 pa stiffness) or (**F**) with 5 μM ML-7 pretreatment for 1 hr. MEFs transfected with TRPC6 reporter were pretreated with 1 μM TG for 1 hr before imaging. MEFs transfected with D3cpv were maintained in Ca^{2+} free HBSS buffer during imaging. "n" represents the cell number in each group. * indicates the significant difference between indicated groups ($P < 0.01$).

NIH-PA Author Manuscript

NIH-PA Author Manuscript

NIH-PA Author Manuscript

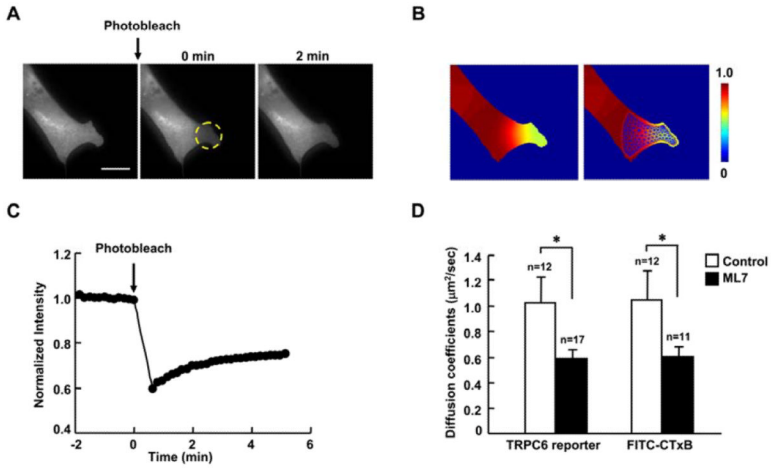

Fig. 5. Reduced intracellular tension decreases the diffusion coefficients of TRPC6 and ganglioside GM1

(**A**) The fluorescence intensity image of a cell expressing TRPC6-YFP before photobleaching (left), and at 0 and 2 min after photobleaching (middle and right), respectively. Yellow broken cycle highlights the region of interest for photobleaching. (**B**) Left: the concentration map after photobleaching (0 min), computed by normalizing the fluorescence intensity with the images before photobleaching. Right: the concentration map overlaid with a triangular mesh generated in the mobile region. (**C**) The time course of fluorescence recovery in the photobleached area as marked in (**A**). (**D**) The estimated diffusion coefficients of TRPC6 and ganglioside GM1 in MEFs transfected with TRPC6-YFP or stained with FITC-CTxB. MEFs were also treated with or without 5 μM ML-7 for 1 hr before FRAP assay. “n” represents the cell number in each group. * indicates the significant difference between indicated groups ($P < 0.05$). Scale bar, 20 μm.

NIH-PA Author Manuscript

NIH-PA Author Manuscript

NIH-PA Author Manuscript

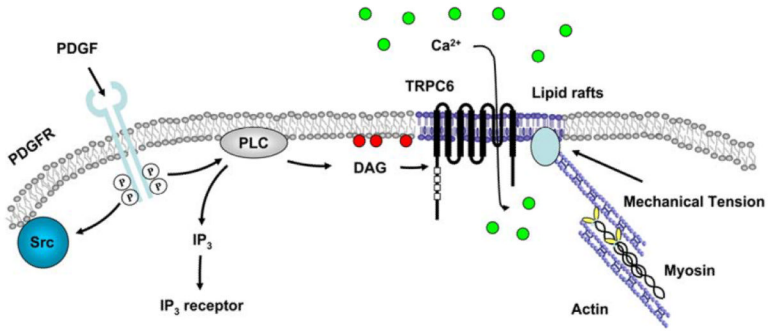

Fig. 6. A proposed signaling network depicting the PDGF induced TRPC6 activation at the plasma membrane

PDGF receptors dimerize upon binding to PDGF and cause the activation of receptor kinase activity. The activated PDGF receptors induce the activation of downstream Src, and PLC which generates IP_3 and DAG. IP_3 activates the IP_3 receptor at ER while DAG can activate TRPC6 at the plasma membrane, specifically on the lipid rafts to induce the Ca^{2+} influx across the plasma membrane. Intercellular tension generated by the actomyosin contractility can affect the interaction between actin cytoskeleton and membrane lipid raft/caveolae microdomains to regulate the structure and function of lipid rafts, which eventually determines the TRPC6 response to PDGF-induced signaling.